

1 **A CRISPR-based SARS-CoV-2 diagnostic assay that is robust against viral**
2 **evolution and RNA editing**

3

4 Kean Hean Ooi^{1,2,4}, Jie Wen Douglas Tay^{1,2,3,4}, Seok Yee Teo^{1,2,3,4}, Mengying Mandy Liu^{1,2},
5 Pornchai Kaewsapsak², Shengyang Jin³, Yong-Gui Gao³, Meng How Tan^{1,2}

6

7 ¹School of Chemical and Biomedical Engineering, Nanyang Technological University,
8 Singapore 637459, Singapore

9 ²Genome Institute of Singapore, Agency for Science Technology and Research, Singapore
10 138672, Singapore

11 ³School of Biological Sciences, Nanyang Technological University, Singapore 637551,
12 Singapore

13 ⁴These authors contributed equally.

14

15 *Correspondence: mh.tan@ntu.edu.sg or tanmh@gis.a-star.edu.sg

16 **Abstract (150 words)**

17

18 Extensive testing is essential to break the transmission of the new coronavirus SARS-CoV-2,
19 which causes the ongoing COVID-19 pandemic. Recently, CRISPR-based diagnostics have
20 emerged as attractive alternatives to quantitative real-time PCR due to their faster turnaround
21 time and their potential to be used in point-of-care testing scenarios. However, existing
22 CRISPR-based assays for COVID-19 have not considered viral genome mutations and RNA
23 editing in human cells. Here, we present the VaNGuard (Variant Nucleotide Guard) test that
24 is not only specific and sensitive for SARS-CoV-2, but can also detect the virus when its
25 genome or transcriptome has evolved or has been edited by deaminases in infected human
26 cells. We show that an engineered AsCas12a enzyme is more tolerant of mismatches than
27 wildtype LbCas12a and that multiplexed Cas12a targeting can overcome the presence of
28 single nucleotide variations. Our assay can be completed in 30 minutes with a dipstick for a
29 rapid point-of-care test.

30

31 **Keywords:** CRISPR; Diagnostics; COVID-19

32

33

34

35 **Introduction**

36

37 COVID-19 is an ongoing global pandemic caused by SARS-CoV-2, a novel coronavirus of
38 zoonotic origin. The outbreak was first reported in Wuhan, China¹⁻³ and has since spread to
39 more than 200 countries in all continents. As of 26 May 2020, there are over 5.4 million
40 confirmed cases and 340,000 deaths worldwide, underscoring the severity of the disease.
41 Importantly, given the high human-to-human transmission potential of SARS-CoV-2
42 including from asymptomatic carriers^{4,6}, rapid and accurate diagnosis is critical for timely
43 treatment and outbreak control. Currently, quantitative real-time PCR (qRT-PCR) is the gold
44 standard method to detect COVID-19. However, it requires specialized and expensive
45 instrumentation to run and thus must be carried out in dedicated facilities with the necessary
46 equipment and expertise. Furthermore, the turnaround time for qRT-PCR is too slow. Even
47 excluding the time it takes to transfer samples from collection points to the test facilities, the
48 PCR process itself will take more than an hour to run. Besides qRT-PCR, serological tests
49 that detect antibodies against SARS-CoV-2 are actively under development. However, such
50 tests have limited practical use for identifying infectious individuals as antibodies are only
51 detectable in later stages of infection when opportunities to treat and limit disease
52 transmission have passed. Hence, there is still an unmet need for rapid, specific, and sensitive
53 point-of-care tests (POCT) for SARS-CoV-2 that are easy to use and can be performed in
54 resource-limited settings.

55

56 CRISPR-Cas has emerged as a powerful technology that can potentially drive next-
57 generation diagnostic platforms. After binding to and cutting a specific target substrate,
58 certain Cas enzymes are then hyperactivated to cleave all neighbouring nucleic acids
59 indiscriminately⁷⁻⁹. By programming the Cas nuclease to recognize desired sequences, such
60 as those containing cancer mutations or from pathogens-of-interest, and providing single-
61 stranded DNA (ssDNA) or RNA reporter molecules in the reaction mix, various groups have
62 successfully developed CRISPR-based diagnostics (CRISPR-Dx) for a range of applications<sup>9-
63 14</sup>. Unsurprisingly, it has also not escaped attention that the same technology can be quickly
64 applied to tackle the ongoing COVID-19 outbreak. Within a few months, nine different
65 CRISPR-based assays have been announced so far (Table 1)¹⁵⁻²³, underscoring the ease-of-
66 use and versatility of the technology.

67

68 While promising, all the existing CRISPR-Dx for COVID-19 have not considered the
69 possibility that the viral sequences may be altered over time or in human cells. Viruses are
70 known to mutate especially under selective pressure. Thousands of SARS-CoV-2 genomes
71 had been sequenced and deposited in the GISAID database^{24,25} and analysis of their
72 sequences revealed numerous mutations, suggesting an ongoing adaptation of the coronavirus
73 to its novel human host²⁶. In particular, mutations had been discovered in the target sites of
74 many current COVID-19 diagnostic tests and could affect the performance of these qRT-PCR
75 tests²⁷. Moreover, mutations in the SARS-CoV-2 genome may also create mismatches in the
76 guide RNA (gRNA) binding site and consequently affect the Cas ribonucleoprotein (RNP)
77 complex's ability to recognize its target. In addition, ADAR and APOBEC deaminases form
78 part of the human host's innate immune responses to viral infection and had recently been
79 shown to edit SARS-CoV-2 RNA²⁸. The respective adenosine-to-inosine and cytosine-to-
80 uracil changes may also affect the ability of the CRISPR-Cas system to detect the virus.

81

82 Here, we report the development of CRISPR-Dx for COVID-19 that incorporate design
83 features that mitigate the loss in signal caused by genomic mutations or RNA editing. We
84 screened several different Cas12a enzymes and found that enAsCas12a, an engineered variant
85 of AsCas12a²⁹, was able to tolerate mismatches at the target site better than wildtype Cas12a
86 nucleases. Furthermore, we demonstrated that incorporation of two gRNAs into the CRISPR-
87 Cas system resulted in partial rescue of the output signal when a variant nucleotide was
88 present in the substrate. Notably, while our assay could tolerate single nucleotide variations
89 in the target sites, it still maintained high specificity and was able to distinguish SARS-CoV-
90 2 from SARS-CoV and MERS-CoV reliably. Taken together, our VaNGuard (Variant
91 Nucleotide Guard) test holds the potential to address the need for a robust and rapid
92 diagnostic assay that will help arrest viral spread and enable worldwide economies to re-open
93 safely in the pandemic.

94

95

96

97

98

99

100

101

103 **Results**

104

105 **Characterization of an existing N-gene gRNA**

106

107 We started off by examining the design of the earliest CRISPR-based assay for COVID-19¹⁵.
108 In this DETECTR assay, wildtype LbCas12a was paired with a 20-nucleotide (nt) gRNA
109 targeting the N-gene of SARS-CoV-2. Given that various Cas12 enzymes had been
110 successfully utilized for human genome engineering, we asked if LbCas12a was the best
111 nuclease to deploy in a diagnostic test. To this end, we purified five different Cas12a
112 enzymes and then paired each one of them with the same gRNA (herein termed N-Mam
113 gRNA) in a fluorescence trans-cleavage assay (Fig. 1a). To assess the feasibility of a
114 CRISPR-based diagnostic assay being deployed in a non-laboratory setting (e.g. a home
115 setting), we carried out the reactions at room temperature using a 500-base pair (bp) synthetic
116 DNA fragment of the SARS-CoV-2 N gene. Fluorescence was monitored over the course of
117 30 minutes in a microplate reader (Supplementary Fig. 1). Expectedly, LbCas12a was able to
118 clearly detect SARS-CoV-2 with no cross-reactivity for SARS-CoV or MERS-CoV at the
119 end of the reaction. Nevertheless, the other four Cas12a enzymes also performed similarly to
120 LbCas12a, with enAsCas12a yielding an even higher fluorescence signal than LbCas12a in
121 the presence of the intended SARS-CoV-2 substrate (Fig. 1b). We also found that the
122 minimum spacer length for the N-Mam gRNA was 20nt, as shortening of the spacer led to a
123 reduction in fluorescence output for all the tested nucleases.

124

125 Next, we tested how mismatches at the gRNA-substrate interface may affect the fluorescence
126 signal. We generated ten new gRNAs targeting the same N-Mam locus, with each harbouring
127 a single point mutation at variable locations along the spacer (Fig. 1c). From the trans-
128 cleavage assay, we observed that LbCas12a was very sensitive to imperfect base pairing
129 between the gRNA and the substrate, as any mismatch along the spacer reduced the
130 fluorescence output to near-background levels (Fig. 1d and Supplementary Fig. 2). In contrast,
131 AsCas12a and its variants were able to tolerate a mismatch 4nt from the 3' end of the gRNA
132 (MM9). Furthermore, we found that enAsCas12a was the most tolerant to mismatches among
133 the five tested enzymes. Hence, our results suggest that enAsCas12a should be paired with
134 the N-Mam gRNA to safeguard against viral mutations or RNA editing at the target site.

135

136 **Evaluation of RT-LAMP parameters**

137

138 To enhance sensitivity, CRISPR-Cas detection is typically combined with an isothermal
139 amplification step, of which there are several options. Due to supply chain issues in the
140 ongoing pandemic, reverse transcription loop-mediated isothermal amplification (RT-
141 LAMP)³⁰ is the method-of-choice for COVID-19 applications. In the DETECTR assay, the
142 RT-LAMP reaction was performed at 62°C for 20–30 minutes¹⁵. Therefore, we first carried
143 out RT-LAMP at 62°C for 20 minutes on synthetic *in vitro*-transcribed (IVT) SARS-CoV-2
144 RNA templates and then used the amplified products in our fluorescence trans-cleavage assay
145 (Fig. 2 and Supplementary Fig. 3). For all the tested enzymes, the viral sequence was
146 consistently and clearly detected in every replicate when 20,000 or more copies of RNA were
147 used as input to RT-LAMP. However, in contrast to the published report¹⁵, when 2,000
148 copies of RNA were used in a 25µl RT-LAMP reaction (i.e. 80 copies per µl) instead, the
149 viral sequence was detected in only around half the replicates for all the Cas enzymes,
150 including LbCas12a.

151

152 Subsequently, we asked how the sensitivity of the CRISPR-based assay would be affected if
153 we varied the parameters of the LAMP reaction (Fig. 2 and Supplementary Fig. 3). When we
154 decreased the duration of LAMP from 20 to 12 minutes, we observed that the fluorescence
155 signal showed an exponential decay with every 10-fold reduction in RNA copy number,
156 indicating that the analytic limit of detection (LoD) became poorer if the amplification step
157 was performed for too short a period of time. Interestingly however, when we increased the
158 reaction temperature from 62°C to 65°C while keeping the duration at 12 minutes, we were
159 able to partially recover the fluorescence signal. Further increase in temperature from 65°C to
160 68°C caused a deterioration in the performance of our CRISPR-Dx (Supplementary Fig. 4).
161 Hence, our results suggest that 65°C is the optimal temperature for LAMP and that the
162 amplification reaction is sensitive to small variations in temperature.

163

164 **Screening of additional gRNAs**

165

166 We wondered if there may be other gRNAs that could yield a stronger fluorescence signal
167 than the N-Mam gRNA in our trans-cleavage assay. The genome of SARS-CoV-2 contains
168 two open reading frames (ORFs), ORF1a and ORF1b, that encode multiple non-structural
169 proteins (nsps), four genes that encode conserved structural proteins (spike protein [S],

170 envelope protein [E], membrane protein [M], and nucleocapsid protein [N]), and several
171 accessory ORFs of unclear function (Fig. 3a)³¹. We aligned the genomes of SARS-CoV-2,
172 SARS-CoV, and MERS-CoV and selected six additional target sites (O1, O2, S1, S2, S3, and
173 N1) that not only contained the necessary TTVV protospacer adjacent motif (PAM) for
174 Cas12a but were also highly divergent between the three coronaviruses (Supplementary Fig.
175 5). We then analysed the collateral activities of our five Cas12a enzymes paired with each of
176 the six new gRNAs over the course of 30 minutes using synthetic DNA fragments of the
177 relevant genes as targets. Curiously, when the N1 gRNA was paired with either wildtype
178 AsCas12a or any of its engineered variants (enAsCas12a, enRR, and enRVR)²⁹, we were able
179 to detect some fluorescence signal even in the absence of template (Fig. 3b and
180 Supplementary Fig. 6), suggesting that AsCas12a may be hyper-activated by certain gRNAs
181 *in vitro* without the need for it to cleave its intended target. Such a phenomenon was not
182 observed with LbCas12a.

183

184 Overall, the three S-gene gRNAs were able to generate similar or higher fluorescence signals
185 than the N-Mam gRNA with the appropriate Cas12a nuclease, while the two O-gene gRNAs
186 generally performed worse. In particular, in the presence of the SARS-CoV-2 target, the
187 collateral activity of LbCas12a complexed with the S3 gRNA was approximately double that
188 of the same enzyme complexed with the N-Mam gRNA (Fig. 3b and Supplementary Fig. 6).
189 There was no cross-reactivity for SARS-CoV or MERS-CoV. We also confirmed that the
190 activity of our own purified protein was comparable to that of a commercially available
191 LbCas12a enzyme used in several recently announced CRISPR-based COVID-19 diagnostic
192 assays^{15,20,21} (Fig. 3c). Subsequently, we investigated the mismatch tolerance of LbCas12a at
193 the S3 target locus but found that collateral activity was greatly diminished for all the
194 mismatched (MM) gRNAs tested (Fig. 3d, e and Supplementary Fig. 7). Hence, although the
195 S3 gRNA may be used in a highly specific assay for known SARS-CoV-2 isolates, it is not
196 ideal for a diagnostic assay that is robust against potential mutations at the target site.

197

198 **Detailed characterization of a new S-gene gRNA**

199

200 Next, we turned our attention to the S2 gRNA. In the presence of the SARS-CoV-2 substrate,
201 this gRNA generated stronger fluorescence signals than the N-Mam gRNA when paired with
202 LbCas12a, AsCas12a, enAsCas12a, or enRVR (Fig. 4a and Supplementary Fig 8). The
203 engineered enAsCas12a enzyme exhibited the highest collateral activity with the S2 gRNA.

204 Importantly, no cross-reactivity for SARS-CoV or MERS-CoV was observed regardless of
205 the Cas12a nuclease used. Furthermore, we found that the minimum spacer length for the S2
206 gRNA was 20nt, as shortening of the spacer reduced the collateral activity of all tested
207 nucleases, although unexpectedly, the 18nt gRNA gave higher fluorescence signals than the
208 19nt gRNA.

209

210 We sought to determine how mismatches at the S2 gRNA-substrate interface may affect the
211 collateral activity of the Cas12a enzymes. To this end, we generated ten additional gRNAs
212 with each harbouring a point mutation at different positions along the spacer (Fig. 4b).
213 Interestingly, we found from the trans-cleavage assay that individual mismatches at the S2
214 locus affected the collateral activity of all the Cas12a endonucleases much less than those at
215 the N-Mam locus (Fig. 4c and Supplementary Fig. 9). Nevertheless, enAsCas12a and enRVR
216 again exhibited the highest tolerance for mismatches, while wildtype LbCas12a was again the
217 most sensitive to imperfect base pairing between the gRNA and its target substrate.

218

219 So far, we had performed the CRISPR-Cas detection at room temperature (24°C) to simulate
220 a non-laboratory setting, but we wondered how the performance of our diagnostic assay
221 would improve if the detection was performed at the optimal temperature (37°C) of the
222 Cas12a enzymes instead. From the trans-cleavage assay, we observed that the fluorescence
223 signal increased approximately twice as fast at 37°C for all tested enzymes in the presence of
224 the intended SARS-CoV-2 template and reached significantly higher levels after 30 minutes
225 of reaction ($P < 0.01$, Student's t-test) (Fig. 4d and Supplementary Fig. 10). There was again
226 no cross-reactivity for SARS-CoV and MERS-CoV. In addition, the activity profile in the
227 presence of point mutations remained similar and in fact even improved slightly for all the
228 nucleases with respect to mismatch tolerance (Fig. 4e and Supplementary Fig. 10). Taken
229 together, our results indicate that our CRISPR-based assay should be performed at 37°C if a
230 faster test result is desired and also suggest that the S2 gRNA is more suitable than the N-
231 Mam gRNA in a diagnostic assay that guards against viral evolution or intracellular RNA
232 editing.

233

234 **Multiplex Cas12a targeting**

235

236 Besides searching for Cas-gRNA pairs that are not only specific for SARS-CoV-2 but are
237 also tolerant of mismatches at the binding site, another strategy to enhance robustness is to

238 incorporate two or more distinct gRNAs into the detection module. As a proof-of-concept, we
239 sought to buffer the collateral activity of LbCas12a, which appeared to be more sensitive to
240 imperfect base pairing at the gRNA-target interface than AsCas12a and its engineered
241 variants. Moreover, LbCas12a protein is commercially available and can be readily bought by
242 diagnostic laboratories that do not have the ability to purify their own enzymes. To keep all
243 the target sites within the same LAMP products, we may pair the S2 gRNA with either the S1
244 or the S3 gRNA, as both worked well with LbCas12a (Fig. 3b and Supplementary Fig. 6). We
245 then tried to design LAMP primers using the online software PrimerExplorer V5. However,
246 we were unable to find any set of primers that would produce an amplicon smaller than
247 500bp that contained both the S2 and S3 loci. In contrast, many primer sets could be obtained
248 for S1 and S2. Hence, we decided to perform our multiplexed targeting experiments with the
249 S1 and S2 gRNAs.

250

251 Using a synthetic DNA fragment of the SARS-CoV-2 S gene as substrate, we first assessed
252 the collateral activity of our five purified Cas12a enzymes when they were combined with
253 both the S1 and S2 gRNAs. All five nucleases exhibited robust activity with perfect matched
254 (PM) gRNAs (Fig. 4f and Supplementary Fig. 11). However, we noted that addition of the S1
255 gRNA caused a small but obvious reduction in the trans-cleavage activity of the three
256 AsCas12a variants, while that of LbCas12a remained approximately the same. This was
257 likely because the S1 gRNA would compete with the S2 gRNA for the Cas proteins but only
258 LbCas12a exhibited strong activity with the S1 gRNA (Fig. 3b and Supplementary Fig. 6).
259 Subsequently, we profiled the activity of the Cas12a nucleases when the S1 PM gRNA was
260 used together with each one of the S2 MM gRNAs (Fig. 4g and Supplementary Fig. 11).
261 Strikingly, we now observed that LbCas12a exhibited the best overall tolerance for
262 mismatches, while AsCas12a and its engineered variants became more sensitive to the
263 mismatches.

264

265 Next, we sought to determine the analytic limit of detection (LoD) of our CRISPR-Dx. We
266 tested three sets of LAMP primers and found one set that amplified well even with low
267 amounts of template (Supplementary Fig. 12). Therefore, we carried out RT-LAMP on
268 synthetic *in vitro*-transcribed (IVT) SARS-CoV-2 RNA templates using this selected primer
269 set. The reaction was performed at 65°C for 15 minutes because we had earlier found the
270 temperature to be optimal for LAMP and we sought to minimize the duration of our
271 diagnostic test. The amplified products were used immediately in our trans-cleavage assay,

272 with the fluorescence monitored over time in a microplate reader (Fig. 5 and Supplementary
273 Fig. 13). When only a single S2 PM gRNA was used, we found that the LoD was around 200
274 copies per reaction for all tested Cas12a nucleases. Expectedly, introduction of a single
275 mismatch (MM10) at the gRNA-substrate interface worsened the sensitivity of CRISPR-Cas
276 detection. More importantly, addition of a S1 PM gRNA was able to partially rescue the
277 mismatch at the S2 locus for LbCas12a, but not for the other Cas12a enzymes. Taken
278 together, our trans-cleavage assays revealed that the use of two gRNAs could increase the
279 robustness of CRISPR-Dx with respect to the presence of variant nucleotides, but care must
280 be taken to only utilize gRNAs that would work well together with the selected Cas nuclease.

281

282 **Towards a point-of-care test**

283

284 To broaden the use cases of our diagnostic assay, we sought to develop a portable point-of-
285 care test (POCT). After the CRISPR-Cas trans-cleavage reaction has taken place, the results
286 can be read out in different ways (Fig. 6a). While a microplate reader is useful for high
287 throughput screening of samples in a centralized facility, it is not amenable to non-laboratory
288 settings like ports of entry, workplaces, schools, public spaces, and homes. Hence, we
289 decided to visualize the results of our assay on a lateral flow strip (Supplementary Fig. 14).
290 Here, the reporter molecule consists of a fluorescent dye (fluorescein) linked to biotin by a
291 short piece of ssDNA. An anti-fluorescein antibody conjugated to gold binds to the dye on
292 the strip. When the viral substrate is absent, the reporter is intact and captured by streptavidin
293 at the control line. However, when the viral target is present, the reporter is cleaved and the
294 fluorescein-antibody complex migrates to the test line where it is captured by an immobilized
295 secondary antibody.

296

297 We performed the RT-LAMP reaction at 65°C for 15 minutes followed by the CRISPR-Cas
298 trans-cleavage reaction at 37°C for 10 minutes before adding a lateral flow strip to the
299 reaction tube. Bands appeared at either the test line or the control line within two minutes
300 (Fig. 6b). Hence, in total, the entire assay took slightly under 30 minutes to complete. Here,
301 we focused on LbCas12a to demonstrate the utility of multiplex targeting. The S2 gRNA (PM
302 or MM10) was used in the assay with or without a second S1 PM gRNA. We also tested
303 different copy numbers of the synthetic SARS-CoV-2 RNA template. Overall, we found that
304 our lateral flow assays gave results that mirrored those from a microplate reader. When the
305 S2 PM gRNA was used alone or in conjunction with the S1 PM gRNA, dark bands appeared

306 at the test line in the presence of at least 200 copies of template in the reaction mix.
307 Expectedly, without any multiplexing, introduction of a mismatch at the S2 gRNA-target
308 interface dramatically reduced the intensity of the test bands and worsened the analytic LoD
309 to 2,000 copies per reaction. Importantly, addition of the S1 PM gRNA was able to partially
310 restore the intensity of the test bands. Quantification of the test and control band intensities
311 further provided a more objective measure of whether the intended target was detected or not.
312 In the case of a mismatch at the S2 locus but perfect base pairing at the S1 locus, we were
313 able to tell that 200 copies per reaction gave a positive test result based on the ratio of the test
314 to control band intensities. In the future, a web or mobile phone application can be developed
315 to distinguish such borderline cases.

316

317 **Discussion**

318

319 There is an urgent healthcare need for rapid and accurate diagnostic tests for COVID-19.
320 What initially started as an infectious disease confined to Wuhan, China has since spread to
321 more than 200 countries worldwide within the span of a few months because SARS-CoV-2
322 has a high potential for human-to-human transmission and the majority of carriers are
323 asymptomatic or only mildly ill. At present, qRT-PCR serves as the gold standard for viral
324 detection, with dozens of test kits available in the market. However, the method requires
325 dedicated instrumentation and trained operators and also has a slow turnaround time. Hence,
326 there is still an unmet need for a rapid, sensitive, specific, and affordable SARS-CoV-2
327 diagnostic assay, which is essential for stopping viral spread and for the safe reopening of
328 economies and schools.

329

330 CRISPR-Dx has the potential to meet society's need for such a diagnostic test. The entire
331 workflow consists of four main modules (Fig. 6a). First is the sample input. Although
332 purified RNA is ideal for performance, the process of RNA extraction will take up precious
333 time, increase cost, and stress the supply chain. Therefore, there is great interest in
334 developing assays that can directly handle patient samples, including nasopharyngeal swabs
335 and saliva. The second module is the isothermal amplification step, which is commonly
336 implemented to enhance the sensitivity of CRISPR-Dx. LAMP³⁰ is the method-of-choice in
337 the current pandemic climate, as its reagents are readily available from several suppliers, but
338 other approaches can also be used, including recombinase polymerase amplification (RPA)³²

339 and helicase-dependent amplification (HDA)³³. The third module is the CRISPR-Cas
340 detection system. Most CRISPR-Dx rely on an indiscriminate collateral activity possessed by
341 some Cas nucleases, including Cas12, Cas13, and Cas14 family members. Lastly, the fourth
342 module is the assay readout. While our work here has demonstrated the use of a microplate
343 reader (for high-throughput testing) and a lateral flow strip (for POCT), another possibility is
344 a graphene-based field-effect transistor, whose high sensitivity has been reported to obviate
345 the need for a pre-amplification step³⁴. Overall, the cost of running a CRISPR-based test per
346 sample is under S\$9 (Table 2), which is around US\$6.40 or €5.80 and is similar to that of an
347 off-the-shelf pregnancy test. The bulk of the cost comes from the LAMP mastermix and the
348 dipstick.

349

350 While promising, current CRISPR-Dx assays for COVID-19 (Table 1) have not taken into
351 account viral evolution and RNA editing. Alarming, mutations in the SARS-CoV-2 genome
352 have been observed at the target sites of multiple existing qRT-PCR diagnostic tests²⁷.
353 Moreover, RNA editing mediated by the ADAR and APOBEC enzymes can also impact
354 upon the performance of COVID-19 diagnostics. Hence, in this work, we sought to bolster
355 the robustness of CRISPR-Dx against unexpected variant nucleotides introduced by
356 evolutionary pressures or RNA editing. Starting from the DETECTR platform^{9,15}, we tested
357 several different natural and engineered Cas12a enzymes and found that enAsCas12a
358 exhibited the highest tolerance for single mismatches at the gRNA-target interface.
359 Importantly, high specificity for SARS-CoV-2 was still maintained with enAsCas12a, as no
360 cross-reactivity for two other closely related coronaviruses SARS-CoV and MERS-CoV was
361 observed. We also screened additional gRNAs and discovered that all the tested nucleases,
362 except enRR, exhibited higher trans-cleavage activity with the S2 gRNA than with the N-
363 Mam gRNA. Hence, our results indicate that enCas12a complexed with the S2 gRNA will
364 serve as a more sensitive and robust SARS-CoV-2 detection system than the published
365 LbCas12a and N-Mam gRNA pair. Nevertheless, we are mindful that enCas12a is not yet a
366 commercially available enzyme. Hence, we demonstrated that a multiplex targeting strategy
367 could also be utilized to enhance the robustness of CRISPR-Dx. For example, the LbCas12a
368 nuclease, which is readily bought, may be combined with both the S1 and S2 gRNAs to
369 increase the robustness of viral detection.

370

371 We note that diagnostic assays can be constructed out of isothermal amplification methods
372 alone without coupling them to a separate CRISPR-Cas detection module. Such assays

373 typically rely on the use of a turbidimeter to measure the extent of magnesium precipitation,
374 labelled primers, or special dyes that sense pH changes, react with amplification by-products,
375 or bind to double-stranded DNA (dsDNA). Due to their relative simplicity, over a dozen
376 LAMP-only diagnostic assays for COVID-19 have been developed so far³⁵⁻⁴⁹. However,
377 isothermal amplification frequently produces spurious non-specific products, which can give
378 rise to false positive results. Although this problem may be circumvented by the use of a
379 sequence-specific detection probe that is distinct from the LAMP primers⁴³, the probe itself is
380 not involved in any amplification process. In contrast, CRISPR-Dx confers two distinct
381 rounds of specificity. The first round comes from primer-specific isothermal amplification
382 such as LAMP, while the second round comes from gRNA-specific Cas detection.
383 Furthermore, the CRISPR-Cas detection system is also capable of signal amplification
384 because each hyperactivated Cas nuclease can proceed to cleave numerous reporter
385 molecules. Hence, CRISPR-Dx can function like a photomultiplier tube and the assay
386 duration can potentially be shortened if all the reagents are in a single-pot and the conditions
387 are optimal for every reaction.

388

389 In conclusion, CRISPR-Dx can serve as a rapid, specific, sensitive, and affordable approach
390 for the detection of SARS-CoV-2. Our work here has further provided two different strategies,
391 namely the use of enCas12a and multiplex targeting, to enhance the robustness of the assay.
392 It can be implemented in a high-throughput format through the use of a microplate reader or
393 deployed as a POCT through the use of a lateral flow strip to enable us to halt viral
394 transmission and reopen our society safely.

395

396

397

398 **Methods**

399

400 **Plasmids and oligonucleotides**

401 The pET28b-T7-Cas12a-NLS-6xHis expression plasmids were gifts from Keith Joung and
402 Benjamin Kleinstiver (Addgene plasmid #114069 [AsCas12a], #114070 [LbCas12a],
403 #114072 [enAsCas12a], #114075 [enRVR], and #114077 [enRR])²⁹. DNA oligonucleotides,
404 custom reporters for the trans-cleavage assays, and gene fragments (ORF1AB, S, and N) for
405 the three coronaviruses SARS-CoV-2, SARS-CoV and MERS-CoV were synthesised by
406 Integrated DNA Technologies. All oligonucleotides used in this study are listed in
407 Supplementary File 1.

408

409 **Cas12a expression and purification**

410 The Cas12a expression plasmids were transformed into *Escherichia coli* BL21 (DE3) and
411 stored as glycerol stocks. Starter cultures were grown in LB broth with 50µg/ml kanamycin at
412 37°C for 16h and diluted 1:50 into 400ml LB-kanamycin broth until an OD₆₀₀ of 0.4-0.6 was
413 reached. Cultures were then induced with 1mM isopropyl β-D-1-thiogalactopyranoside
414 (IPTG) and incubated at 25°C for another 16h. Subsequently, cells were harvested by
415 centrifugation at 3,220g for 20min and resuspended in lysis buffer [50mM HEPES, 500mM
416 NaCl, 2mM MgCl₂, 20mM imidazole, 1% Triton X-100, 1mM DTT, 0.005mg/ml lysozyme
417 (Vivantis), 1X Halt Protease Inhibitor Cocktail (Thermo Fisher Scientific)], followed by
418 sonication at high power for 10 cycles of 30s ON/OFF (Bioruptor Plus; Diagenode). Lysates
419 were clarified by centrifugation at 10,000g for 15min. The supernatants were pooled, loaded
420 onto a gravity flow column packed with Ni-NTA agarose (Qiagen), and rotated for 2h at 4°C.
421 The column was washed twice with 5ml wash buffer (50mM Tris, 300mM NaCl and 30mM
422 imidazole). Five elutions were performed with 500µl elution buffer (50mM Tris, 300mM
423 NaCl, and 200mM imidazole) and analysed by SDS-PAGE. The final gel filtration step was
424 performed with a HiLoad 16/600 Superdex 200pg column (GE Healthcare) on a fast protein
425 liquid chromatography purification system (ÄKTA Explorer; GE Healthcare), which was
426 eluted with storage buffer (50mM Tris, 300mM NaCl, and 1mM DTT). Fractions containing
427 Cas12a were collected, analysed by SDS-PAGE, and concentrated to around 500µl with
428 Vivaspin 20, 50,000 MWCO concentrator units (Sartorius). Glycerol was added to a final
429 concentration of 20%. Protein concentrations were measured with the Quick Start Bradford

430 Protein Assay (Bio-Rad) aliquoted, and stored at -80°C. For comparison, EnGen Lba Cas12a
431 was purchased from New England Biolabs (NEB).

432

433 **gRNA design**

434 Complete genomes of SARS-CoV-2 (accession MN908947.3), SARS-CoV (accession
435 NC_004718.3), and MERS-CoV (accession NC_019843.3) were retrieved from NCBI
436 (<https://www.ncbi.nlm.nih.gov/>) and aligned with MUSCLE
437 (<https://www.ebi.ac.uk/Tools/msa/muscle/>) using default settings. Potential target sites (20nt
438 spacers) in the ORF1AB, S, and N genes were selected from non-conserved regions
439 containing a TTTV PAM. Potential targets were filtered after a specificity check on BLASTn
440 (<https://blast.ncbi.nlm.nih.gov/Blast.cgi>) to remove non-specific candidates. Truncated
441 gRNAs were generated by shortening their spacers to 18nt and 19nt lengths at the 3' end.

442

443 ***In vitro* transcription (IVT) of gRNAs**

444 Templates for gRNA synthesis were designed with the following sequence order: T7
445 promoter-Cas12a scaffold-spacer. Top strand DNA oligos consisting of the T7 promoter (5'-
446 TAATACGACTCACTATAGG-3') and scaffold (5'-TAATTTCTACTCTTGTAGAT-3' for
447 AsCas12a and its variants; 5'-AATTTCTACTAAGTG TAGAT-3' for LbCas12a) were
448 annealed to the bottom strand and extended by Q5 High-Fidelity DNA polymerase (NEB).
449 IVT of the dsDNA products was performed with the HiScribe T7 Quick High Yield RNA
450 Synthesis kit (NEB) at 37°C overnight. Following DNase I digestion, gRNAs were purified
451 with the RNA Clean & Concentrator-5 kit (ZYMO Research), analysed by 2% TAE-agarose
452 gel electrophoresis to assess RNA integrity, measured with NanoDrop 2000, and stored at -
453 20°C.

454

455 **Synthesis of DNA and RNA templates**

456 Gene fragments (gBlocks) were cloned into pCR-Blunt II-TOPO vector using the Zero Blunt
457 TOPO PCR Cloning kit (Invitrogen) and their sequences were verified by Sanger sequencing.
458 The vectors were used as templates for PCR with Q5 High-Fidelity DNA polymerase (NEB)
459 and the products were gel extracted and purified with the PureNA Biospin Gel Extraction kit
460 (Research Instruments). DNA concentrations were measured using NanoDrop 2000 and all
461 the DNA samples were stored at 4°C. To generate RNA templates for RT-LAMP assays, the
462 forward primers used for PCR were appended with the T7 promoter sequence. After PCR

463 amplification with the gBlock-TOPO vectors as template, IVT was performed as described
464 for gRNA generation.

465

466 **Fluorescence trans-cleavage assay**

467 Cas ribonucleoprotein (RNP) complexes were pre-assembled with 65nM AsCas12a/
468 LbCas12a, 195nM gRNA, and 200nM custom ssDNA fluorophore-quencher (FQ) reporter in
469 reaction buffer (1X NEBuffer 3.1 plus 0.4mM DTT) for 30 minutes at room temperature.
470 Subsequently, the cleavage reaction was initiated by adding 3nM DNA template
471 (approximately 1E11 copies) to a total volume of 50 μ l and then transferred to a 96-well
472 microplate (Costar). Fluorescence intensities were measured with either the Infinite M1000
473 Pro (Tecan) or the Spectramax M5 plate reader (Molecular Devices) for 30 minutes at room
474 temperature, with measurement intervals of 5 minutes (λ_{ex} : 485 nm; λ_{em} : 535 nm).

475

476 **RT-LAMP reaction**

477 Synthetic SARS-CoV-2 RNA templates were serially diluted and amplified by RT-LAMP
478 using the WarmStart LAMP Kit (NEB). LAMP primers were added to a final concentration
479 of 0.2 μ M for F3 and B3, 1.6 μ M for FIP and BIP, and 0.8 μ M for LF and LB. The optimal
480 temperature for RT-LAMP was found to be 65°C. Subsequently, 4 μ l RT-LAMP products
481 were used as templates for the trans-cleavage assay, instead of 3nM PCR-amplified DNA
482 template.

483

484 **Lateral flow readout**

485 500nM of custom ssDNA biotin reporter was used instead of the FQ reporter. The Cas12a
486 detection reaction was performed at 37°C for 10 minutes. Subsequently, 50 μ L HybriDetect
487 assay buffer (Milenia Biotec) was added to the reaction and a HybriDetect (Milenia Biotec)
488 dipstick was inserted directly into the solution in an upright position. The dipstick was
489 incubated in the reaction for 2 minutes at room temperature before inspection.

490

491

492

493 **Acknowledgements**

494 This work is supported by an Industry Alignment Fund – Pre-positioning Programme grant
495 from the Agency for Science, Technology and Research (H18/01/a0/019 to MHT), a Ministry
496 of Education Academic Research Fund Tier 1 grant (2017-T1-001-214 to MHT), an Open
497 Fund - Individual Research Grant from the National Medical Research Council
498 (NMRC/OFIRG/0017/2016 to MHT), and core funding from the Genome Institute of
499 Singapore (to MHT). The authors also thank Xin Ning Nicole Tang for help with setting up
500 the CRISPR diagnostics workflow and members of the DaRE lab for discussions.

501

502 **Authors' contributions**

503 M.H.T conceived the project and provided overall supervision. K.H.O., J.W.D.T., S.Y.T., and
504 M.H.T. designed the experiments. K.H.O., J.W.D.T., S.Y.T., M.M.L., and P.K. performed the
505 experiments. S.J. and Y.-G.G. assisted with protein purification. K.H.O., J.W.D.T., S.Y.T.,
506 and M.H.T. analysed the data. M.H.T. wrote the manuscript with inputs from K.H.O.,
507 J.W.D.T., and S.Y.T. All authors approved the manuscript.

508

509 **Additional information**

510 **Supplementary Information** accompanies this paper

511 **Competing interests:** The authors declare that they have no competing interests.

512

513

514

515

516 **Tables**

517

518 **Table 1.** List of CRISPR-based assays for COVID-19 that have been announced (as of 26 May 2020).

Name	DETECTR	CARMEN	CASdetec	STOPCovid	CRISPR-nCoV	CRISPR-Detection	AIOD-CRISPR	FELUDA	CREST
Status	Published ¹⁵	Published ¹⁶	Published ¹⁷	MedRxiv preprint ¹⁸	MedRxiv preprint ¹⁹	BioRxiv preprint ²⁰	BioRxiv preprint ²¹	BioRxiv preprint ²²	BioRxiv preprint ²³
Enzyme	LbCas12a	LwCas13a	AapCas12b	AapCas12b	LwCas13a	LbCas12a	LbCas12a	FnCas9	LwCas13a
Based on collateral activity	Yes	Yes	Yes	Yes	Yes	Yes	Yes	No	Yes
Validated on patient samples	Yes (N = 11)	No	No	Yes (N = 12)	Yes (N = 52)	No	No	Yes (N = 1)	No
Affiliated company	Mammoth (partnering with GSK)	-	-	Sherlock	-	CASPR	-	Tata Sons	-

519

520

521 **Table 2.** Estimated cost of CRISPR-Dx for each sample.

Reagent	Approximate Price (\$)	Number of Reactions	Price per reaction (\$)	
			Plate reader	Dipstick
RNA extraction kit	1,200	90,800	0.01	0.01
IVT Kit	491	22,700	0.02	0.02
RT-LAMP mastermix	1,489	500	2.98	2.98
Cleavage assay buffer	41	1,000	0.04	0.04
LbCas12a	450	600	0.75	0.75
LAMP primer (F3)	5	1,200	<0.01	<0.01
LAMP primer (B3)	5	1,200	<0.01	<0.01
LAMP primer (FIP)	10	125	0.08	0.08
LAMP primer (BIP)	10	125	0.08	0.08
LAMP primer (LF)	5	300	0.02	0.02
LAMP primer (LB)	5	300	0.02	0.02
FITC-quencher reporter	315	650	0.48	-
96-well plate	8	96	0.08	-
FITC-biotin reporter	200	5,555	-	0.04
Dipstick	490	100	-	4.90
TOTAL			4.58	8.94

522

523

524 **Figure Legends**

525

526 **Fig. 1** Activity and mismatch tolerance of various Cas12a enzymes with the N-Mam gRNA.

527 **a** Schematic of a fluorescence trans-cleavage assay. Here, the reporter comprises a
528 fluorophore linked to a quencher by a short piece of ssDNA. The gRNA is programmed to
529 recognize a particular locus of the SARS-CoV-2 genome. In the absence of the virus, the
530 reporter molecule is intact and thus no fluorescence is observed. However, when the virus is
531 present, the Cas12a RNP will bind to and cleave its programmed target, become
532 hyperactivated, and cut the ssDNA linker between the fluorophore and quencher, thereby
533 generating a fluorescence signal.

534 **b** Fluorescence measurements using a microplate reader after 30 minutes of cleavage reaction.
535 1E11 copies of DNA template corresponding to one of the coronaviruses (see colour bar)
536 were present in a 50µl reaction. Spacers of three different lengths targeting the N-Mam locus
537 were tested. There was no cross-reactivity for SARS-CoV or MERS-CoV as expected. All
538 the measurements were normalized to the no-template control (NTC) at the start of the
539 experiment. Data represent mean ± s.e.m. (n = 3 biological replicates).

540 **c** Sequences of perfect matched (PM) or mismatched (MM) spacers targeting the N-Mam
541 locus. Each mismatched position is indicated by a bold red letter.

542 **d** Heatmap showing the tolerance of various Cas12a enzymes to mismatched N-Mam gRNAs.
543 The fluorescence readings are scaled between 0 and 1, where 1 is the highest measurement
544 obtained and 0 is the background signal for NTC at the start of the experiment.

545

546 **Fig. 2** Analytic limit of detection (LoD) under various LAMP reaction conditions. Different
547 copies of synthetic SARS-CoV-2 RNA fragments were used as input and the volume of each
548 RT-LAMP reaction was 25µl. The fluorescence readings here were taken after 10 minutes of
549 cleavage reaction. Data represent mean ± s.e.m. (62°C for 20min: n = 4-7 biological
550 replicates; 62°C/ 65°C for 12min: n = 3 biological replicates).

551

552 **Fig. 3** Collateral activity of various Cas12a enzymes complexed with different gRNAs.

553 **a** Organization of the SARS-CoV-2 genome. ORF1a and ORF1b occupy over half of the
554 genome. Genes encoding structural proteins are indicated by green boxes, while genes
555 encoding accessory proteins are indicated by cyan boxes. Although ORF10 is annotated in
556 the genome, there is currently no evidence of its expression⁵⁰. The locations of the new

557 gRNAs are shown by pink bars below the genes, while the N-Mam locus is shown by a red
558 bar.

559 **b** Fluorescence measurements using a microplate reader after 30 minutes of cleavage reaction.
560 1E11 copies of the relevant DNA target were present in a 50µl reaction. All the readings were
561 normalized to the negative control (NTC) at the start of the experiment. The N1 gRNA gave
562 an unexpected result, whereby it triggered the collateral activity of AsCas12a and its variants
563 even in the absence of a template. Data represent mean ± s.e.m. (n = 3-6 biological replicates).

564 **c** Visualization of cleavage reactions for the S3 gRNA using a UV transilluminator.
565 Transition of colours from blue to yellow to red indicates an increasing amount of collateral
566 activity.

567 **d** Sequences of perfect matched (PM) or mismatched (MM) spacers targeting the S3 locus.
568 Each mismatched position is indicated by a bold red letter.

569 **e** Collateral activity of LbCas12a complexed with perfect matched or mismatched S3 gRNA.
570 The fluorescence measurements were taken after 30 minutes of cleavage reaction using a
571 microplate reader and all the readings were normalized to the NTC at the start of the
572 experiment. Our results indicate that LbCas12a should be paired with the S3 gRNA instead of
573 the N-Mam gRNA if a diagnostic assay that is highly specific for known SARS-CoV-2
574 isolates is desired. Data represent mean ± s.e.m. (n = 3 biological replicates).

575

576 **Fig. 4** Activity and mismatch tolerance of various Cas12a enzymes with the S2 gRNA.

577 **a** Fluorescence measurements for a single S2 gRNA after 30 minutes of trans-cleavage
578 reaction at 24°C. 1E11 copies of DNA template corresponding to one of the three
579 coronaviruses (see colour bar) were present in a 50µl reaction. Spacers of three different
580 lengths targeting the S2 locus were tested. All the measurements were normalized to the
581 negative control (NTC) at the 0min timepoint. No cross-reactivity for SARS-CoV or MERS-
582 CoV was detected. Unexpectedly, the 18nt spacer yielded higher fluorescence than the 19nt
583 spacer for all the tested nucleases, especially LbCas12a. Data represent mean ± s.e.m. (n = 3-
584 4 biological replicates).

585 **b** Sequences of perfect matched (PM) or mismatched (MM) spacers targeting the S2 locus.
586 Each mismatched position is indicated by a bold red letter.

587 **c** Heatmap showing the tolerance of various Cas12a enzymes to mismatched S2 gRNAs
588 when the trans-cleavage assay was performed at 24°C. The fluorescence readings are scaled
589 between 0 and 1 (variable shades of green), where 1 is the highest measurement obtained at
590 24°C and 0 is the background signal for NTC at the start of the experiment.

591 **d** Fluorescence measurements for a single S2 gRNA after 30 minutes of trans-cleavage
592 reaction at 37°C. There was still no cross-reactivity for SARS-CoV or MERS-CoV at the
593 higher temperature, but the fluorescence signal for SARS-CoV-2 was approximately twice as
594 high. Data represent mean \pm s.e.m. (n = 3 biological replicates).

595 **e** Heatmap showing the tolerance of various Cas12a enzymes to mismatched S2 gRNAs
596 when the trans-cleavage assay was performed at 37°C. The fluorescence readings are scaled
597 between 0 and 1 (variable shades of red), where 1 is the highest measurement obtained at
598 37°C and 0 is the background signal for NTC at the start of the experiment. The most
599 detrimental mismatch position appears to be 2nt from the PAM-distal end (MM10).

600 **f** Fluorescence measurements for two PM gRNAs (S1 and S2) after 30 minutes of cleavage
601 reaction at 37°C. No cross-reactivity for SARS-CoV or MERS-CoV was observed. Data
602 represent mean \pm s.e.m. (n = 3 biological replicates).

603 **g** Heatmap showing how the addition of a second perfect matched S1 gRNA changed the
604 tolerance of various Cas12a enzymes to mismatched S2 gRNAs. The trans-cleavage assay
605 was performed at 37°C, with the fluorescence readings scaled between 0 and 1.

606

607 **Fig. 5** Analytic LoD for gRNAs targeting the S-gene. Different copies of *in vitro* transcribed
608 SARS-CoV-2 RNA fragments were used as input to the RT-LAMP reaction, which was
609 performed at 65°C for 15 minutes. The Cas detection reaction was then carried out at 37°C,
610 with the fluorescence measurements here taken after 10 minutes using a microplate reader.
611 Data represent mean \pm s.e.m. (n = 3-5 biological replicates).

612

613 **Fig. 6** Implementation of our VaNGuard assay on lateral flow strips.

614 **a** Overview of a prototypical CRISPR-Dx workflow. While a microplate reader can allow up
615 to 96 samples to be processed at once, it is not amenable to point-of-care testing. In contrast,
616 a lateral flow strip proves a simple visual readout akin to an off-the-shelf pregnancy test.

617 **b** Detection of SARS-CoV-2 sequence using gRNAs targeting the S-gene. Different copies of
618 synthetic SARS-CoV-2 RNA fragments were used as input to the RT-LAMP reaction, which
619 was performed at 65°C for 15 minutes. Next, the Cas detection reaction was carried out at
620 37°C for 10 minutes before a dipstick was added to each reaction tube. The bands on the
621 dipstick appeared by 2 minutes. In total, the VaNGuard assay was completed in under 30
622 minutes.

623 **References**

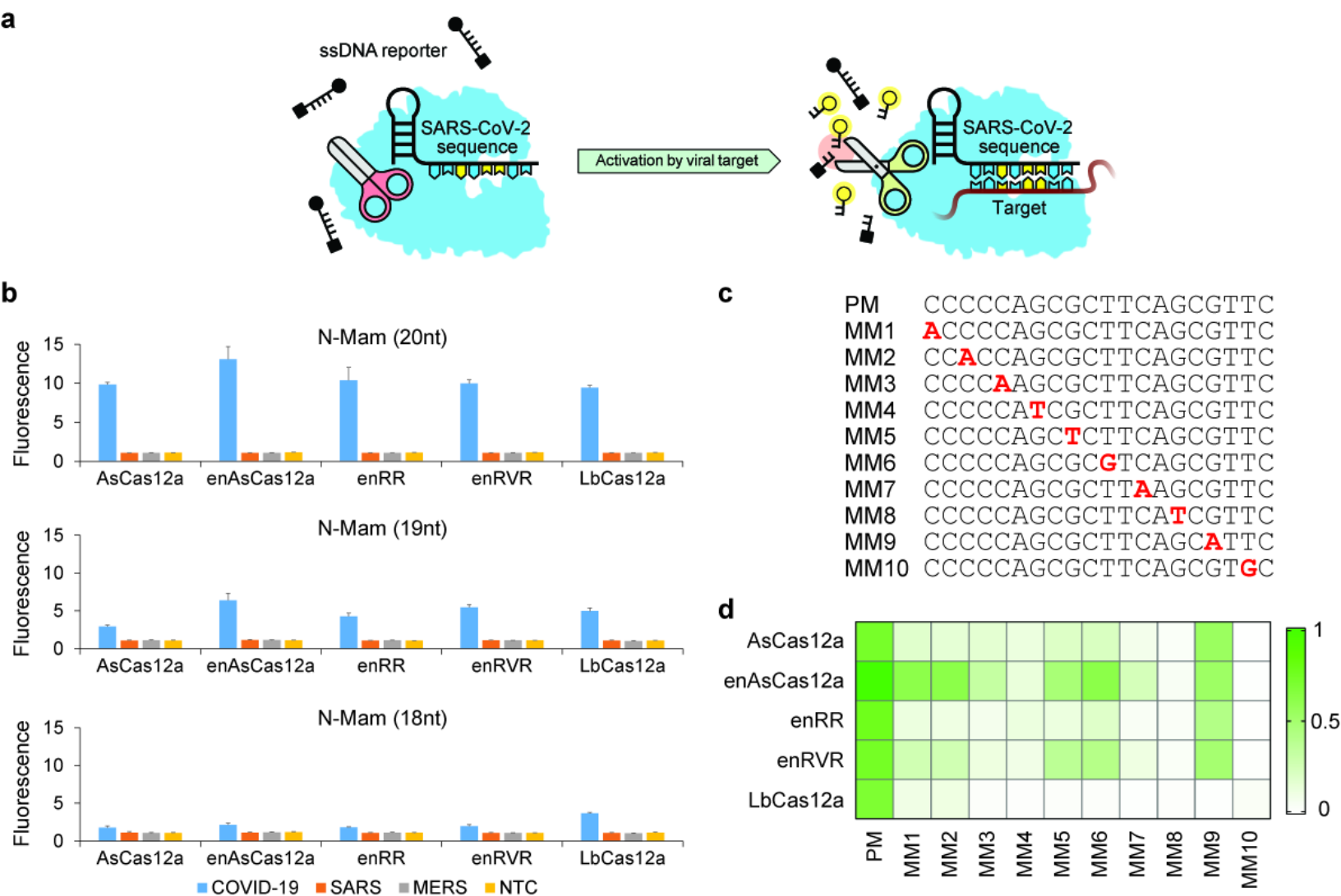
624

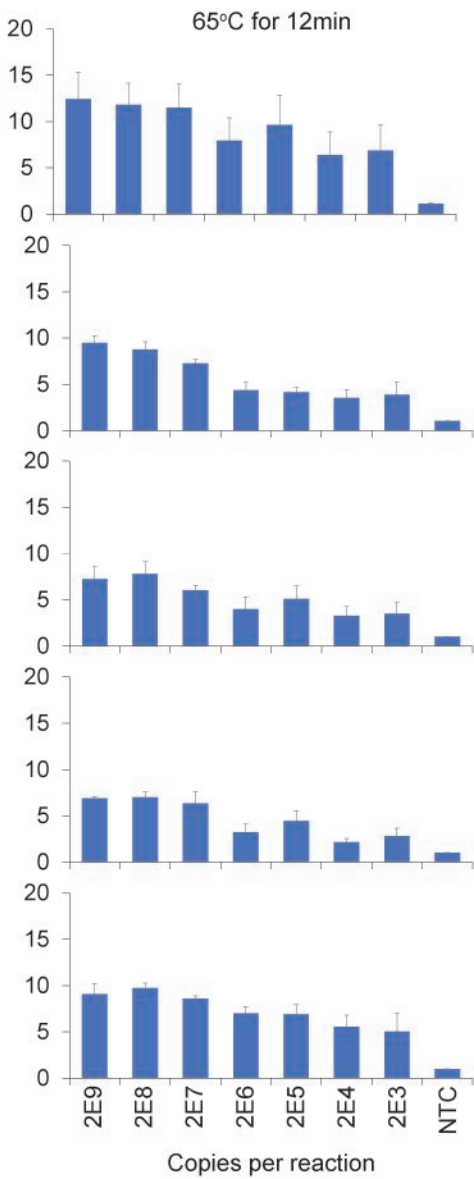
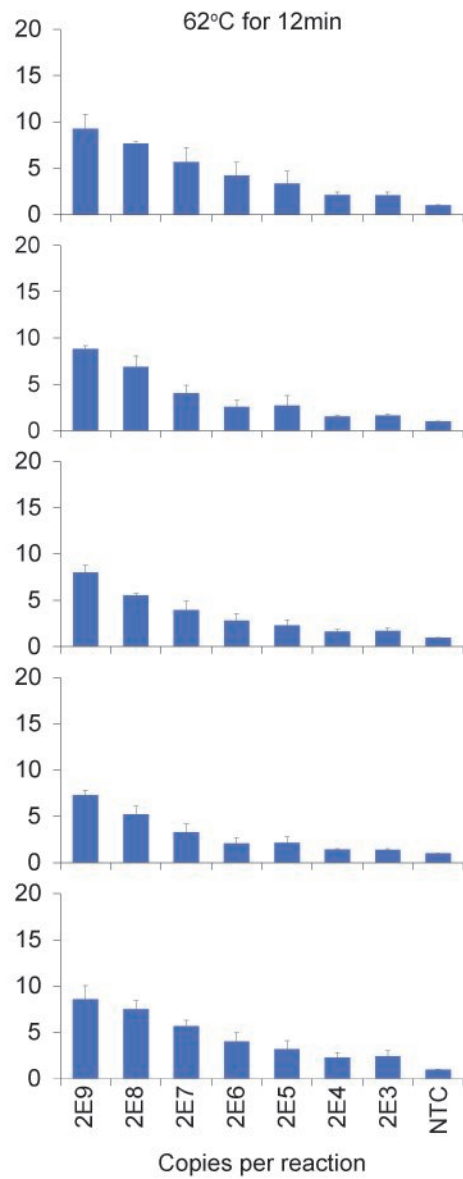
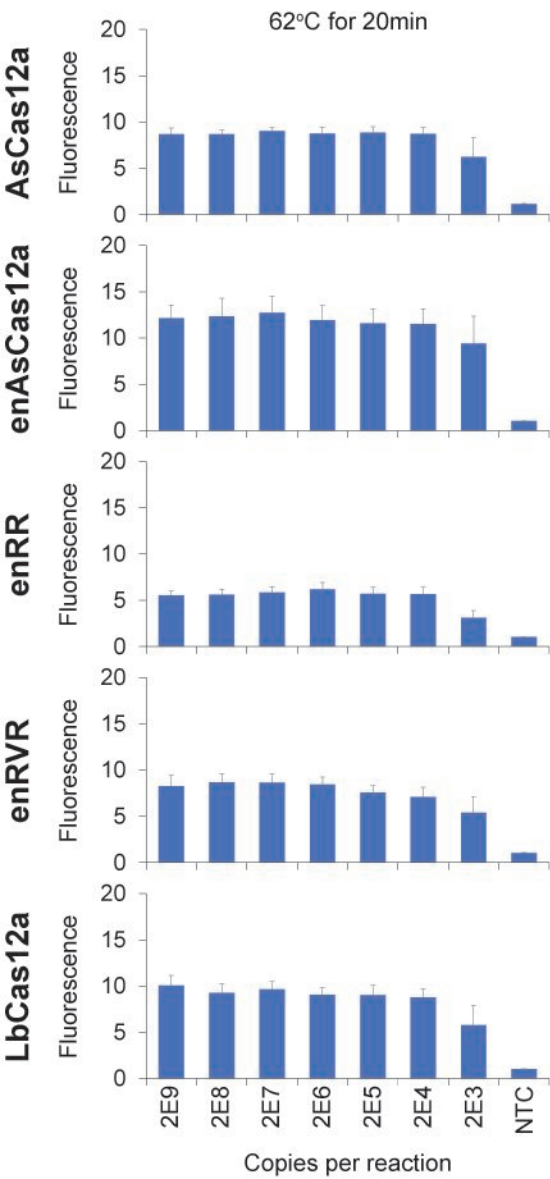
- 625 1 Zhou, P. *et al.* A pneumonia outbreak associated with a new coronavirus of probable
626 bat origin. *Nature* **579**, 270-273, doi:10.1038/s41586-020-2012-7 (2020).
- 627 2 Zhu, N. *et al.* A Novel Coronavirus from Patients with Pneumonia in China, 2019. *N*
628 *Engl J Med* **382**, 727-733, doi:10.1056/NEJMoa2001017 (2020).
- 629 3 Wang, C., Horby, P. W., Hayden, F. G. & Gao, G. F. A novel coronavirus outbreak of
630 global health concern. *Lancet* **395**, 470-473, doi:10.1016/S0140-6736(20)30185-9
631 (2020).
- 632 4 Li, Q. *et al.* Early Transmission Dynamics in Wuhan, China, of Novel Coronavirus-
633 Infected Pneumonia. *N Engl J Med* **382**, 1199-1207, doi:10.1056/NEJMoa2001316
634 (2020).
- 635 5 Bai, Y. *et al.* Presumed Asymptomatic Carrier Transmission of COVID-19. *JAMA*,
636 doi:10.1001/jama.2020.2565 (2020).
- 637 6 Rothe, C. *et al.* Transmission of 2019-nCoV Infection from an Asymptomatic Contact
638 in Germany. *N Engl J Med* **382**, 970-971, doi:10.1056/NEJMc2001468 (2020).
- 639 7 Abudayyeh, O. O. *et al.* C2c2 is a single-component programmable RNA-guided
640 RNA-targeting CRISPR effector. *Science* **353**, aaf5573, doi:10.1126/science.aaf5573
641 (2016).
- 642 8 East-Seletsky, A. *et al.* Two distinct RNase activities of CRISPR-C2c2 enable guide-
643 RNA processing and RNA detection. *Nature* **538**, 270-273, doi:10.1038/nature19802
644 (2016).
- 645 9 Chen, J. S. *et al.* CRISPR-Cas12a target binding unleashes indiscriminate single-
646 stranded DNase activity. *Science* **360**, 436-439, doi:10.1126/science.aar6245 (2018).
- 647 10 Gootenberg, J. S. *et al.* Nucleic acid detection with CRISPR-Cas13a/C2c2. *Science*
648 **356**, 438-442, doi:10.1126/science.aam9321 (2017).
- 649 11 Gootenberg, J. S. *et al.* Multiplexed and portable nucleic acid detection platform with
650 Cas13, Cas12a, and Csm6. *Science* **360**, 439-444, doi:10.1126/science.aaq0179
651 (2018).
- 652 12 Harrington, L. B. *et al.* Programmed DNA destruction by miniature CRISPR-Cas14
653 enzymes. *Science* **362**, 839-842, doi:10.1126/science.aav4294 (2018).

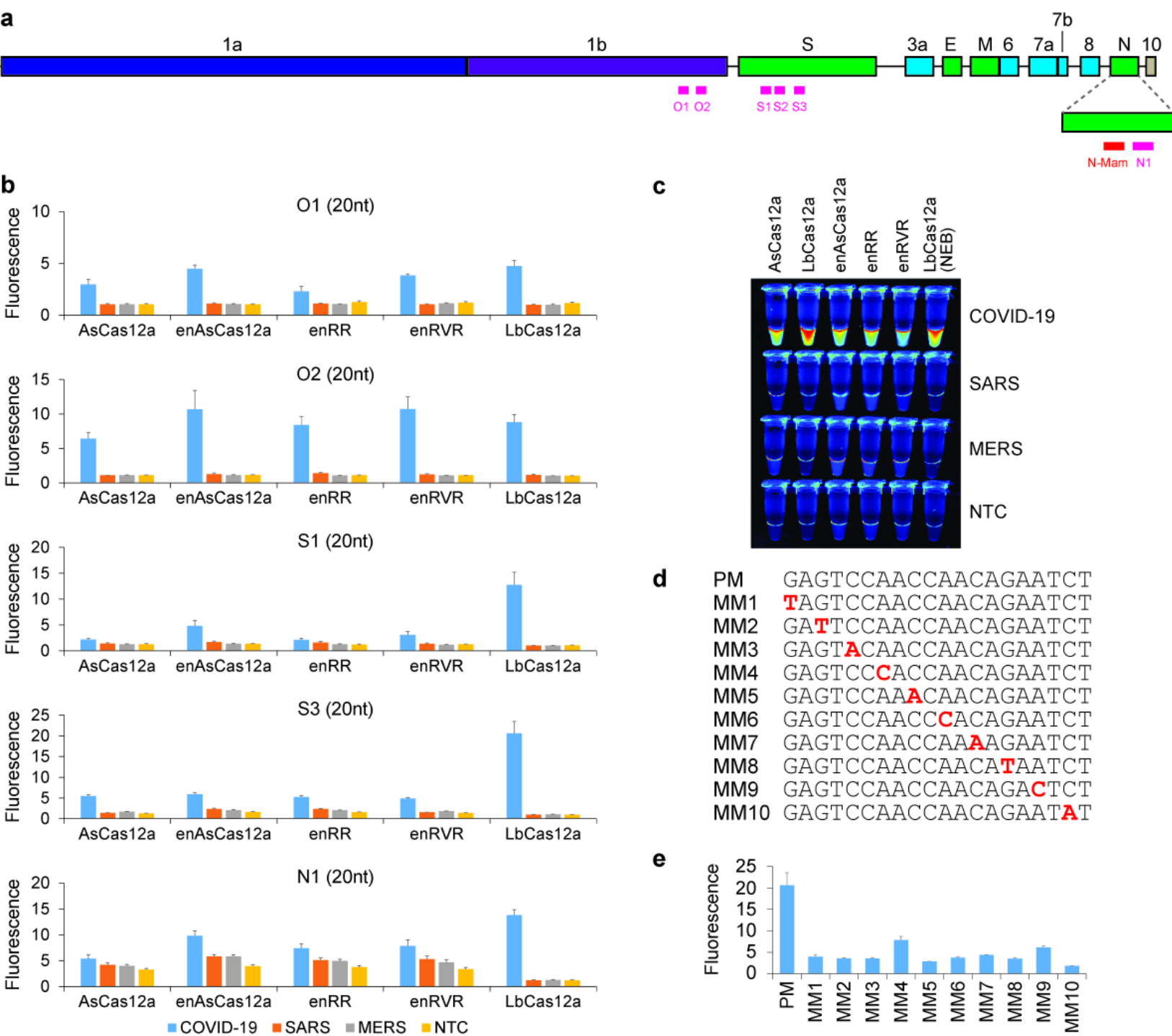
- 654 13 Teng, F. *et al.* CDetection: CRISPR-Cas12b-based DNA detection with sub-attomolar
655 sensitivity and single-base specificity. *Genome Biol* **20**, 132, doi:10.1186/s13059-019-
656 1742-z (2019).
- 657 14 Myhrvold, C. *et al.* Field-deployable viral diagnostics using CRISPR-Cas13. *Science*
658 **360**, 444-448, doi:10.1126/science.aas8836 (2018).
- 659 15 Broughton, J. P. *et al.* CRISPR-Cas12-based detection of SARS-CoV-2. *Nat*
660 *Biotechnol*, doi:10.1038/s41587-020-0513-4 (2020).
- 661 16 Ackerman, C. M. *et al.* Massively multiplexed nucleic acid detection using Cas13.
662 *Nature*, doi:10.1038/s41586-020-2279-8 (2020).
- 663 17 Guo, L. *et al.* SARS-CoV-2 detection with CRISPR diagnostics. *Cell Discov* **6**, 34,
664 doi:10.1038/s41421-020-0174-y (2020).
- 665 18 Joung, J. *et al.*, doi:10.1101/2020.05.04.20091231 (2020).
- 666 19 Hou, T. *et al.*, doi:10.1101/2020.02.22.20025460 (2020).
- 667 20 Lucia, C., Federico, P.-B. & Alejandra, G. C., doi:10.1101/2020.02.29.971127 (2020).
- 668 21 Ding, X., Yin, K., Li, Z. & Liu, C., doi:10.1101/2020.03.19.998724 (2020).
- 669 22 Azhar, M. *et al.*, doi:10.1101/2020.04.07.028167 (2020).
- 670 23 Rauch, J. N. *et al.*, doi:10.1101/2020.04.20.052159 (2020).
- 671 24 Elbe, S. & Buckland-Merrett, G. Data, disease and diplomacy: GISAID's innovative
672 contribution to global health. *Glob Chall* **1**, 33-46, doi:10.1002/gch2.1018 (2017).
- 673 25 Shu, Y. & McCauley, J. GISAID: Global initiative on sharing all influenza data -
674 from vision to reality. *Euro Surveill* **22**, doi:10.2807/1560-7917.ES.2017.22.13.30494
675 (2017).
- 676 26 van Dorp, L. *et al.* Emergence of genomic diversity and recurrent mutations in SARS-
677 CoV-2. *Infect Genet Evol* **83**, 104351, doi:10.1016/j.meegid.2020.104351 (2020).
- 678 27 Wang, R., Hozumi, Y., Yin, C. & Wei, G.-W. Mutations on COVID-19 diagnostic
679 targets. *arXiv e-prints*, arXiv:2005.02188 (2020).
680 <https://ui.adsabs.harvard.edu/abs/2020arXiv200502188W>.
- 681 28 Di Giorgio, S., Martignano, F., Torcia, M. G., Mattiuz, G. & Conticello, S. G.
682 Evidence for host-dependent RNA editing in the transcriptome of SARS-CoV-2.
683 *Science Advances*, doi:10.1126/sciadv.abb5813 (2020).
- 684 29 Kleinstiver, B. P. *et al.* Engineered CRISPR-Cas12a variants with increased activities
685 and improved targeting ranges for gene, epigenetic and base editing. *Nat Biotechnol*
686 **37**, 276-282, doi:10.1038/s41587-018-0011-0 (2019).

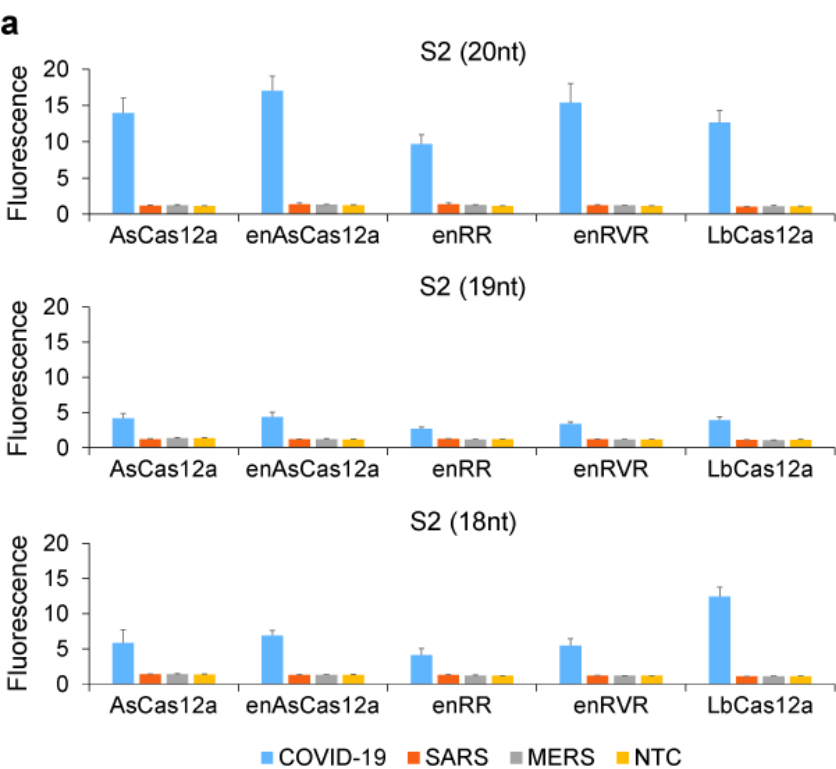
- 687 30 Notomi, T. *et al.* Loop-mediated isothermal amplification of DNA. *Nucleic Acids Res*
688 **28**, E63, doi:10.1093/nar/28.12.e63 (2000).
- 689 31 Wu, A. *et al.* Genome Composition and Divergence of the Novel Coronavirus (2019-
690 nCoV) Originating in China. *Cell Host Microbe* **27**, 325-328,
691 doi:10.1016/j.chom.2020.02.001 (2020).
- 692 32 Piepenburg, O., Williams, C. H., Stemple, D. L. & Armes, N. A. DNA detection using
693 recombination proteins. *PLoS Biol* **4**, e204, doi:10.1371/journal.pbio.0040204 (2006).
- 694 33 Vincent, M., Xu, Y. & Kong, H. Helicase-dependent isothermal DNA amplification.
695 *EMBO Rep* **5**, 795-800, doi:10.1038/sj.embor.7400200 (2004).
- 696 34 Hajian, R. *et al.* Detection of unamplified target genes via CRISPR-Cas9 immobilized
697 on a graphene field-effect transistor. *Nat Biomed Eng* **3**, 427-437,
698 doi:10.1038/s41551-019-0371-x (2019).
- 699 35 Lu, R. *et al.* Development of a Novel Reverse Transcription Loop-Mediated
700 Isothermal Amplification Method for Rapid Detection of SARS-CoV-2. *Virolog Sin*,
701 doi:10.1007/s12250-020-00218-1 (2020).
- 702 36 Baek, Y. H. *et al.* Development of a reverse transcription-loop-mediated isothermal
703 amplification as a rapid early-detection method for novel SARS-CoV-2. *Emerg*
704 *Microbes Infect* **9**, 998-1007, doi:10.1080/22221751.2020.1756698 (2020).
- 705 37 Huang, W. E. *et al.* RT-LAMP for rapid diagnosis of coronavirus SARS-CoV-2.
706 *Microb Biotechnol*, doi:10.1111/1751-7915.13586 (2020).
- 707 38 Yan, C. *et al.* Rapid and visual detection of 2019 novel coronavirus (SARS-CoV-2)
708 by a reverse transcription loop-mediated isothermal amplification assay. *Clin*
709 *Microbiol Infect* **26**, 773-779, doi:10.1016/j.cmi.2020.04.001 (2020).
- 710 39 Sun, F. *et al.* Smartphone-based multiplex 30-minute nucleic acid test of live virus
711 from nasal swab extract. *Lab Chip* **20**, 1621-1627, doi:10.1039/d0lc00304b (2020).
- 712 40 Yu, L. *et al.* Rapid detection of COVID-19 coronavirus using a reverse transcriptional
713 loop-mediated isothermal amplification (RT-LAMP) diagnostic platform. *Clin Chem*,
714 doi:10.1093/clinchem/hvaa102 (2020).
- 715 41 Park, G. S. *et al.* Development of Reverse Transcription Loop-Mediated Isothermal
716 Amplification Assays Targeting Severe Acute Respiratory Syndrome Coronavirus 2. *J*
717 *Mol Diagn*, doi:10.1016/j.jmoldx.2020.03.006 (2020).
- 718 42 Song, J., Bau, H. H. & El-Tholoth, M., doi:10.26434/chemrxiv.11860137.v1.
- 719 43 Bhadra, S., Riedel, T. E., Lakhotia, S., Tran, N. D. & Ellington, A. D.,
720 doi:10.1101/2020.04.13.039941 (2020).

- 721 44 Lalli, M. A. *et al.*, doi:10.1101/2020.05.07.20093542 (2020).
- 722 45 Lamb, L. E., Bartolone, S. N., Ward, E. & Chancellor, M. B.,
723 doi:10.1101/2020.02.19.20025155 (2020).
- 724 46 Zhang, Y. *et al.*, doi:10.1101/2020.02.26.20028373 (2020).
- 725 47 Ben-Assa, N. *et al.*, doi:10.1101/2020.04.22.20072389 (2020).
- 726 48 Dao Thi, V. L. *et al.*, doi:10.1101/2020.05.05.20092288 (2020).
- 727 49 Butler, D. J. *et al.*, doi:10.1101/2020.04.20.048066 (2020).
- 728 50 Kim, D. *et al.* The Architecture of SARS-CoV-2 Transcriptome. *Cell* **181**, 914-921
729 e910, doi:10.1016/j.cell.2020.04.011 (2020).
- 730









b

PM	ACTCCTGGTGATTCTTCTTC
MM1	CCTCCTGGTGATTCTTCTTC
MM2	ACGCCTGGTGATTCTTCTTC
MM3	ACTCA ^T GGTGATTCTTCTTC
MM4	ACTCCT ^T GTGATTCTTCTTC
MM5	ACTCCTGG ^G GATTCTTCTTC
MM6	ACTCCTGGTG ^C TTCTTCTTC
MM7	ACTCCTGGTGAT ^G CTTCTTC
MM8	ACTCCTGGTGATT ^C GTTCTTC
MM9	ACTCCTGGTGATTCTT ^A ATTC
MM10	ACTCCTGGTGATTCTTCT ^G C

